Oncolytic virus-mediated reducing of myeloid-derived suppressor cells enhances the efficacy of PD-L1 blockade in gemcitabine-resistant pancreatic cancer

Yoshinori Kajiwara[1], Hiroshi Tazawa[1,2], Motohiko Yamada[1], Nobuhiko Kanaya[1], Takuro Fushimi[1], Satoru Kikuchi[1], Shinji Kuroda[1], Toshiaki Ohara[1,3], Kazuhiro Noma[1], Ryuichi Yoshida[1], Yuzo Umeda[1], Yasuo Urata[4], Shunsuke Kagawa[1], Toshiyoshi Fujiwara[1]

[1] Department of Gastroenterological Surgery, and [3] Department of Pathology and Experimental Medicine, Okayama University Graduate School of Medicine, Dentistry and Pharmaceutical Sciences, Okayama 700-8558, Japan.
[2] Center for Innovative Clinical Medicine, Okayama University Hospital, Okayama 700-8558, Japan.
[4] Oncolys BioPharma Inc., Tokyo 105-001, Japan.

Materials and Methods

Figure S1
Comparison of GEM resistance and PD-L1 expression
In parental and GEM-resistant PDAC tumors.

Figure S2
Comparison of the expression of 40 cytokines
between P and GR PAN02 conditioned medium using a cytokine array.

Figure S3
Increased proportions of MDSCs and granulocytic MDSCs
among BMDCs incubated with GR PAN02 CM.

Figure S4
Increased proliferation of and proportion of PD-L1$^+$ MDSCs and decreased proliferation of CD8$^+$ T cells
among BMDCs incubated with GR PAN02 CM.

Figure S5
Relative viability of GR PAN02 cells after treatment with GM-CSF or anti-GM-CSF antibody for 3 days.

Figure S6
Decreased proportion of granulocytic MDSCs, decreased proliferation of MDSCs,
and increased proliferation of CD8$^+$ T cells among GR PAN02 CM-incubated BMDCs
after OBP-702 treatment.

Figure S7
Relative cell viability of BMDCs and MDSCs after treatment with OBP-301 or OBP-702 for 3 days.

Figure S8
In vivo antitumor effect of OBP-301 and OBP-702 against GR PAN02 tumors.

Figure S9
In vivo antitumor effect of PD-L1 blockade and OBP-702
in monotherapy or combination therapy against GR PAN02 tumors.

Materials and Methods

MDSC proliferation assay

MDSCs were isolated from the spleens of healthy 6- to 8-week-old female C57BL/6J mice using a mouse MDSC isolation kit (130-094-538; Miltenyi Biotec, Auburn, CA, USA) and then labeled with CFSE (Invitrogen, Carlsbad, CA, USA). The CFSE-labeled MDSCs were cultured in parental or GEM-resistant PAN02 CM or culture medium containing GM-CSF (40 ng/mL). After incubation for 4 days, MDSC proliferation was assessed by measuring the proportion of $CFSE^-$ cells using a flow cytometry (BD FACSLyric; BD Biosciences).

T-cell suppression assay

$CD8^+$ T cells were isolated from the spleens of healthy 6- to 8-week-old female C57BL/6J mice using a mouse $CD8^+$ isolation kit (130-104-075; Miltenyi Biotec), and labeled with CFSE. The CFSE-labeled $CD8^+$ T cells were incubated in 24-well plates with CD3/CD28 beads (11456D; Thermo Fisher Scientific, Waltham, MA, USA) and MDSCs induced by parental or GEM-resistant PAN02 CM. After incubation for 4 days, the cells were stained with anti-CD8 antibody, and the CFSE fluorescence intensity of the $CD8^+$ T cells was examined using a flow cytometry (BD FACSLyric; BD Biosciences).

Isolation of MDSCs

BMDCs were derived from healthy 6- to 8-week-old female C57BL/6J mice and incubated with GEM-resistant PAN02 CM. After incubation for 4 days, cells were collected and stained with Fixable Dye (423102; BioLegend, San Diego, CA, USA), anti-CD11b antibody (101206; BioLegend), and anti-Gr1 antibody (108436; BioLegend). The proportion of $CD11b^+Gr1^+$ MDSCs was determined by flow cytometry (BD FACSAria III cell sorter; BD Biosciences) according to the manufacturer's protocol. Cell purity (> 97%) and viability were assessed by flow cytometry (BD FACSLyric; BD Biosciences).

Cell viability assay

Cells were seeded in 96-well plates at a density of 1×10^3 cells/well (PAN02) or 1×10^4 cells/well (BMDC, MDSC). Cells were treated with recombinant GM-CSF at 0, 1, 5, 10, 50, or 100 ng/mL or anti-GM-CSF neutralizing antibody at 0, 1, 5, 10, 50, or 100 μg/mL or infected with OBP-301 or OBP-702 at a MOI of 0, 1, 5, 10, 50, or 100 PFUs/cell. Cell viability was determined 3 days after treatment using TACS® XTT Cell Proliferation Assay (R&D Systems, Minneapolis, MN, USA) according to the manufacturer's protocol.

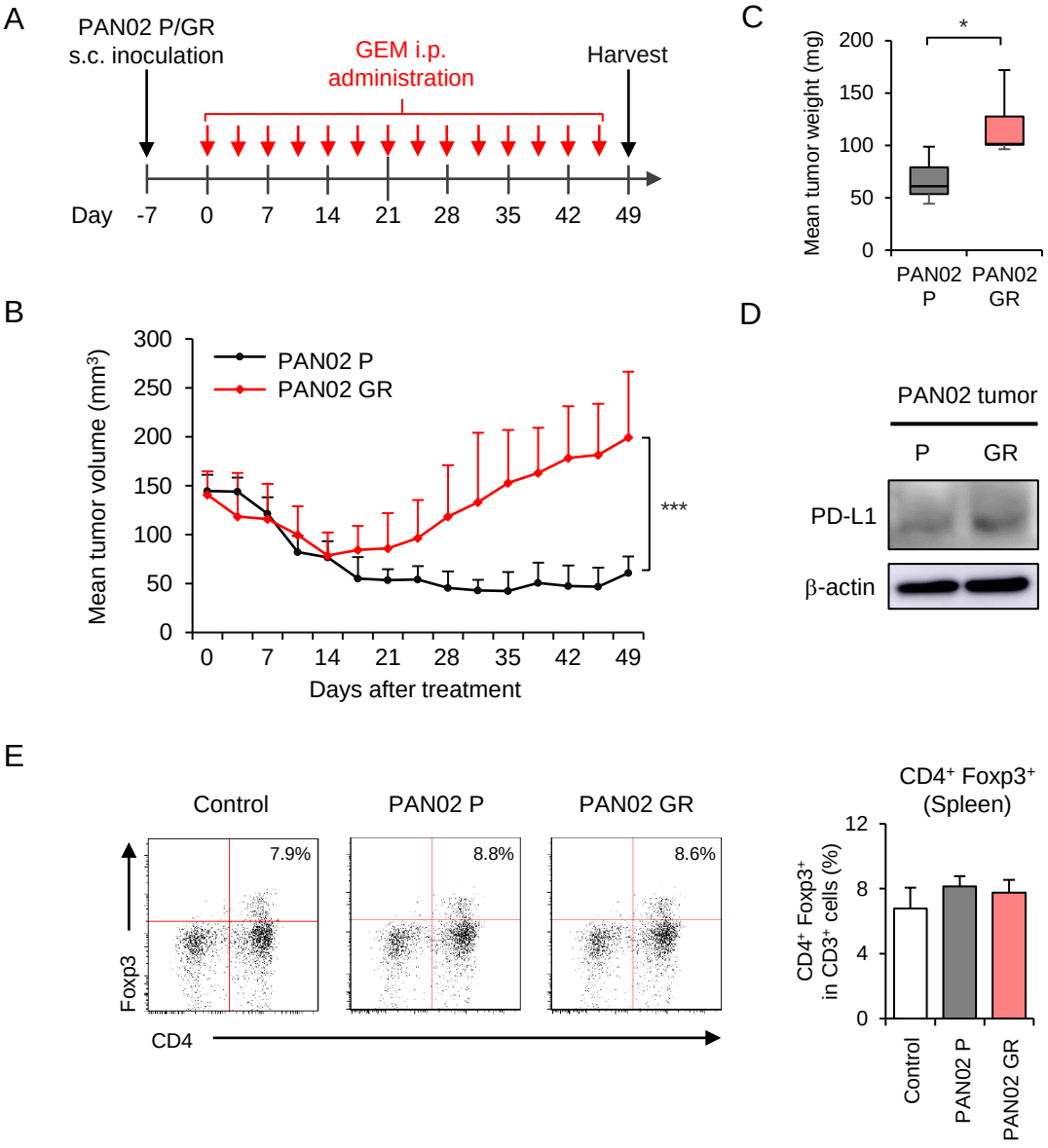

Supplementary Fig. S1. Comparison of GEM resistance and PD-L1 expression in parental and GEM-resistant PAN02 tumors. A, Parental (P) and GEM-resistant (GR) PAN02 cells (4×10^6 cells) were subcutaneously (s.c.) inoculated into the flanks of C57BL/6J mice. Seven days after inoculation, a 100-μL volume of solution containing gemcitabine (GEM, 100 mg/kg) was intraperitoneally (i.p.) administered twice a week for 7 weeks (red arrows). **B** and **C**, Growth curves (**B**) and weight (**C**) of P and GR PAN02 tumors are shown. **D**, Expression of PD-L1 protein in P and GR PAN02 tumors. β-Actin was used as a loading control. **E**, Representative data of flow cytometric analysis for CD4 and Foxp3. The percentage of $CD4^+Foxp3^+$ Treg cells among $CD3^+$ cells is shown. Data are expressed as mean ± SD (n = 5 in each group; *, $P < 0.05$; ***, $P < 0.001$).

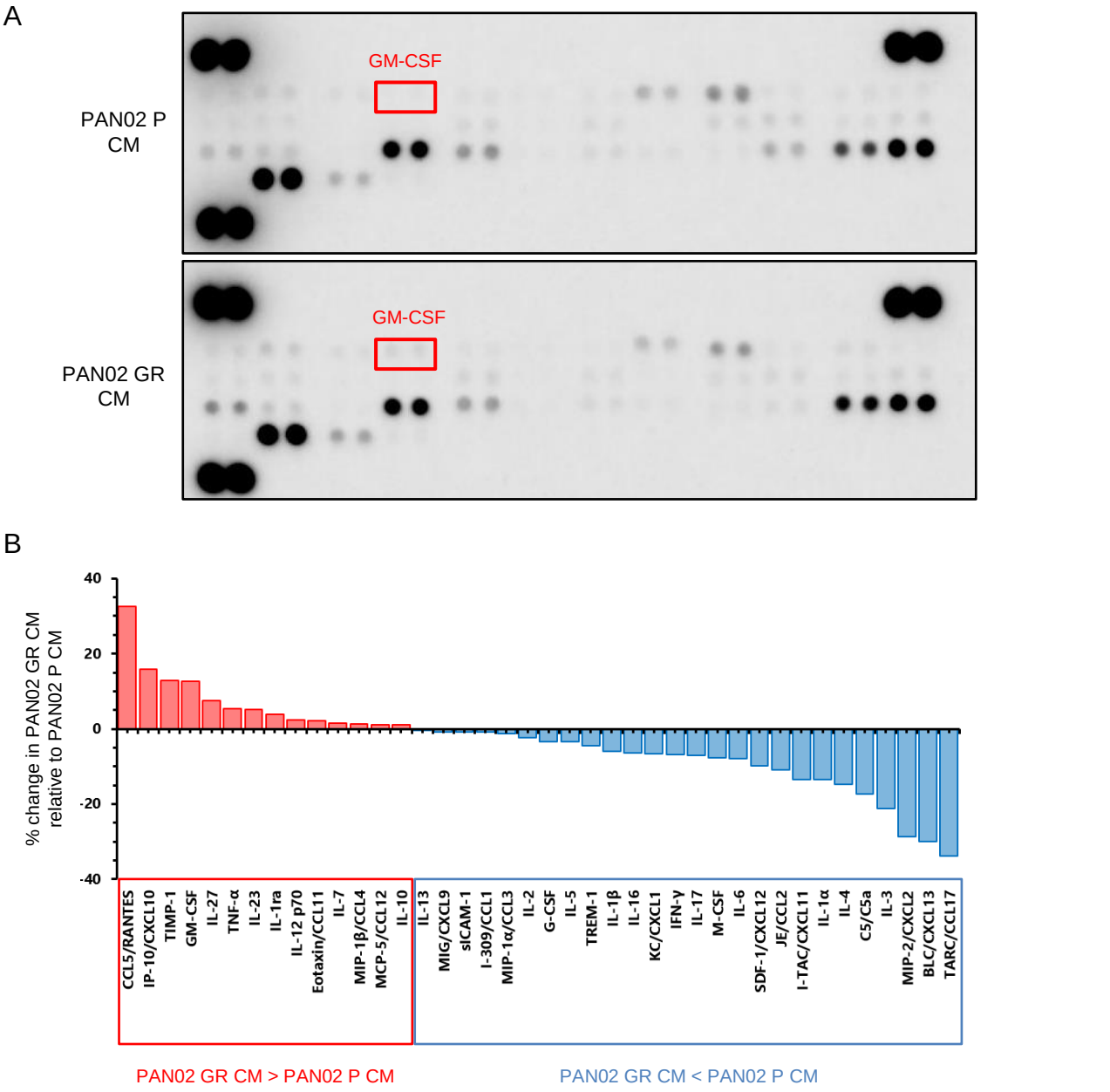

Supplementary Fig. S2. Comparison of the expression of 40 cytokines between P and GR PAN02 conditioned medium using a cytokine array. A, Data of cytokine array using conditioned medium (CM) from P and GR PAN02 cells. **B**, Percent change in levels of 40 cytokines in GR PAN02 CM relative to P PAN02 CM. Among 40 cytokines, the expression of 14 was upregulated and 26 downregulated in GR PAN02 CM compared with P PAN02 CM, indicated by red and blue boxes, respectively.

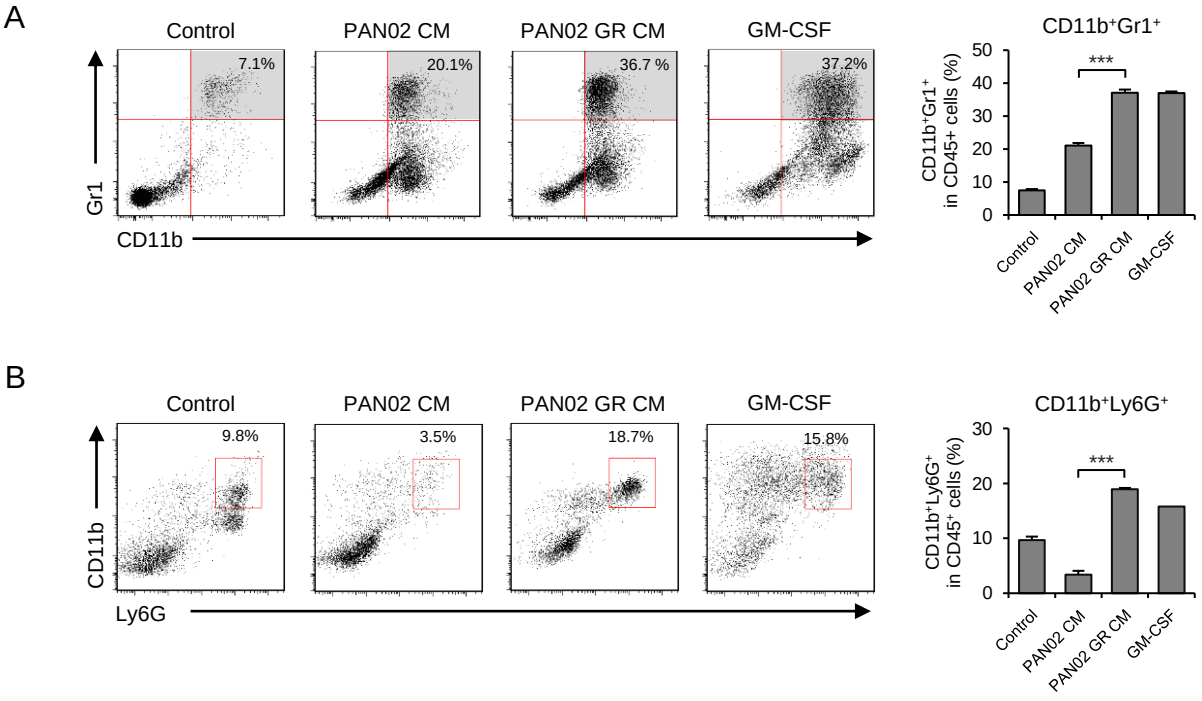

Supplementary Fig. S3. Increased proportions of MDSCs and granulocytic MDSCs among BMDCs incubated with GR PAN02 CM. A, **B**, Representative data of flow cytometric analysis of CD11b, Gr1, and Ly6G in each group. The percentages of $CD11b^+Gr1^+$ MDSCs and $CD11b^+Ly6G^+$ granulocytic MDSCs among $CD45^+$ cells are shown. Data are expressed mean ± SD (n = 3 in each group; ***, $P < 0.001$).

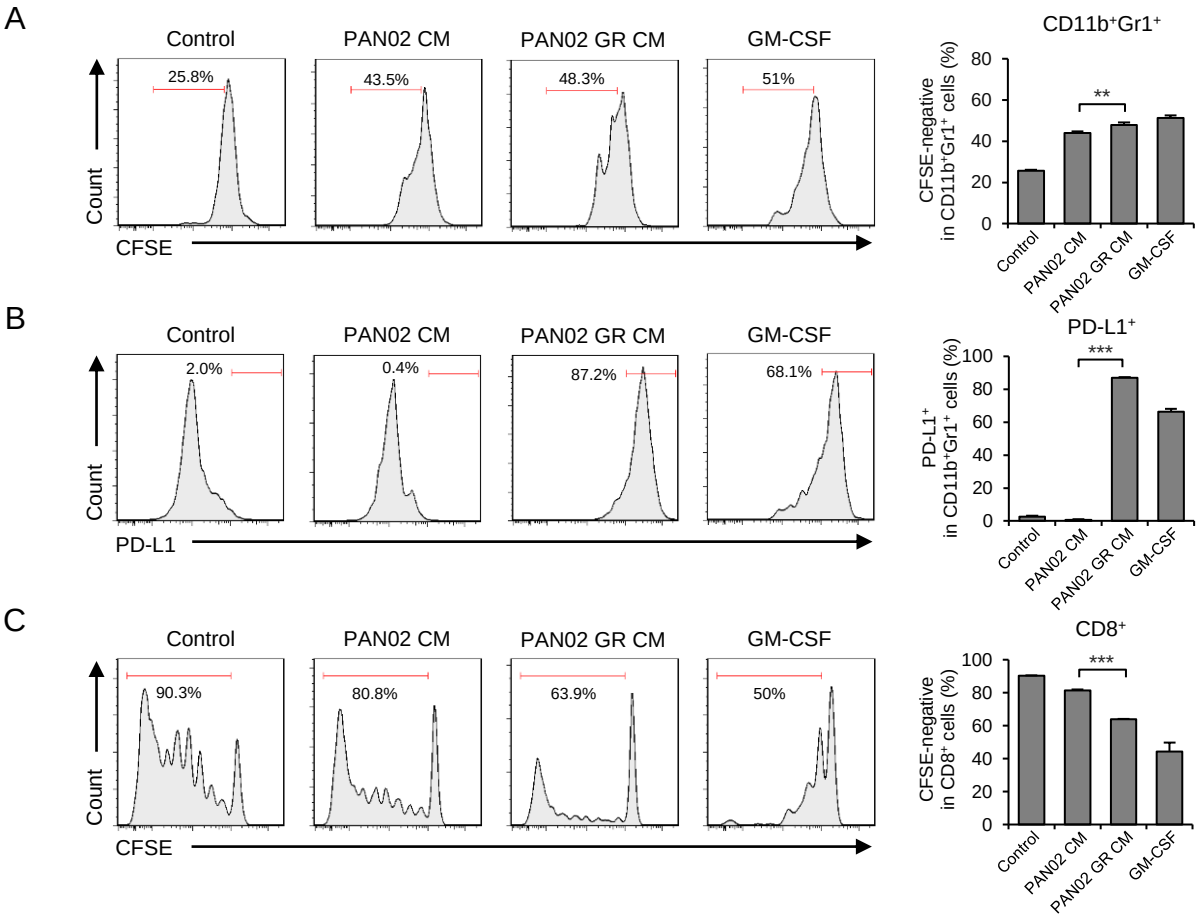

Supplementary Fig. S4. Increased proliferation and proportion of PD-L1$^+$ MDSCs and decreased proliferation of CD8$^+$ T cells among BMDCs incubated with GR PAN02 CM.

A, **B**, **C**, Representative data of flow cytometric analysis for CFSE or PD-L1 in each group. The proportions of CFSE$^-$ (**A**) and PD-L1$^+$ (**B**) cells among CD11b$^+$Gr1$^+$ MDSCs and the proportion of CFSE$^-$ cells (**C**) among CD8$^+$ T cells are shown. Data are expressed mean ± SD (n = 3 in each group; **, $P < 0.01$; ***, $P < 0.001$).

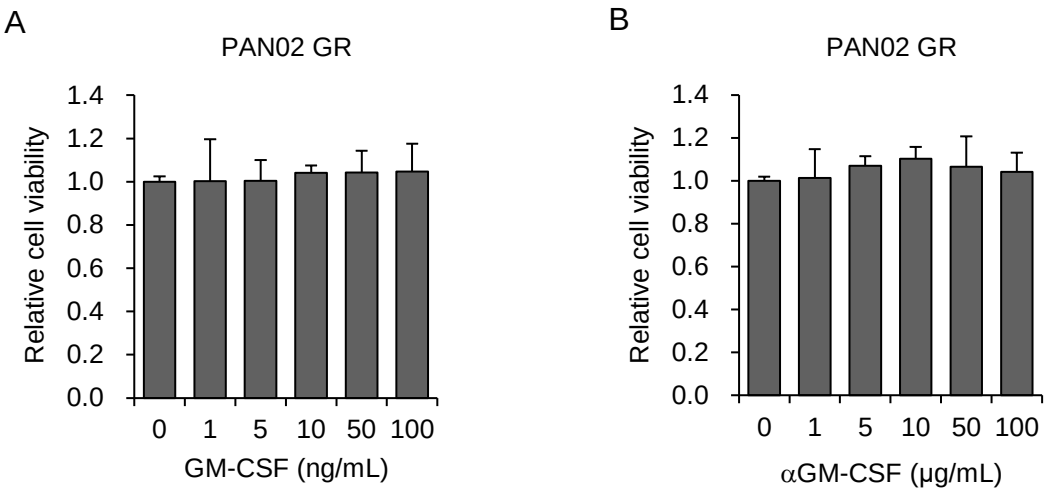

Supplementary Fig. S5. Relative viability of GR PAN02 cells after treatment with GM-CSF or anti-GM-CSF antibody for 3 days. A, **B**, GR PAN02 cells seeded in 96-well plates were treated with recombinant GM-CSF (**A**) or anti-GM-CSF neutralizing antibody (**B**) at the indicated doses for 72 h. Cell viability was quantified using the XTT assay and calculated relative to that of non-treated cells, which was set at 1.0. Cell viability data are expressed as mean ± SD (n = 5).

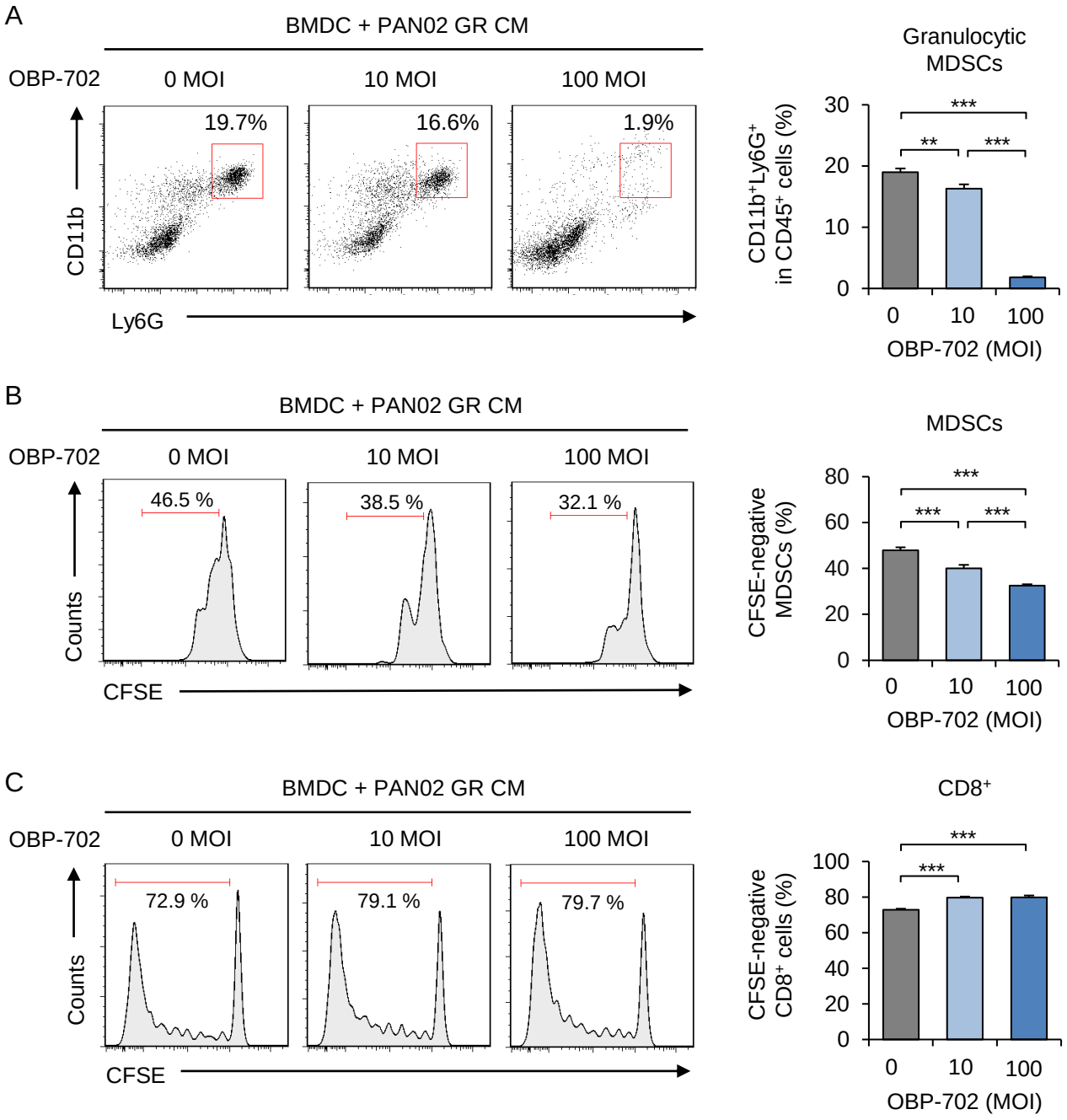

Supplementary Fig. S6. Decreased proportion of granulocytic MDSCs, decreased proliferation of MDSCs, and increased proliferation of CD8$^+$ T cells among GR PAN02 CM-incubated BMDCs after OBP-702 treatment. A, **B**, **C**, Representative data of flow cytometric analysis for Ly6G, CD11b, and CFSE in each group. The proportion of CD11b$^+$Ly6G$^+$ cells (**A**) among CD45$^+$ cells and the proportion of CFSE$^-$ cells among MDSCs (**B**) or CD8$^+$ T cells (**C**) are shown. Data are expressed as mean ± SD (n = 3 in each group; **, $P < 0.01$; ***, $P < 0.001$).

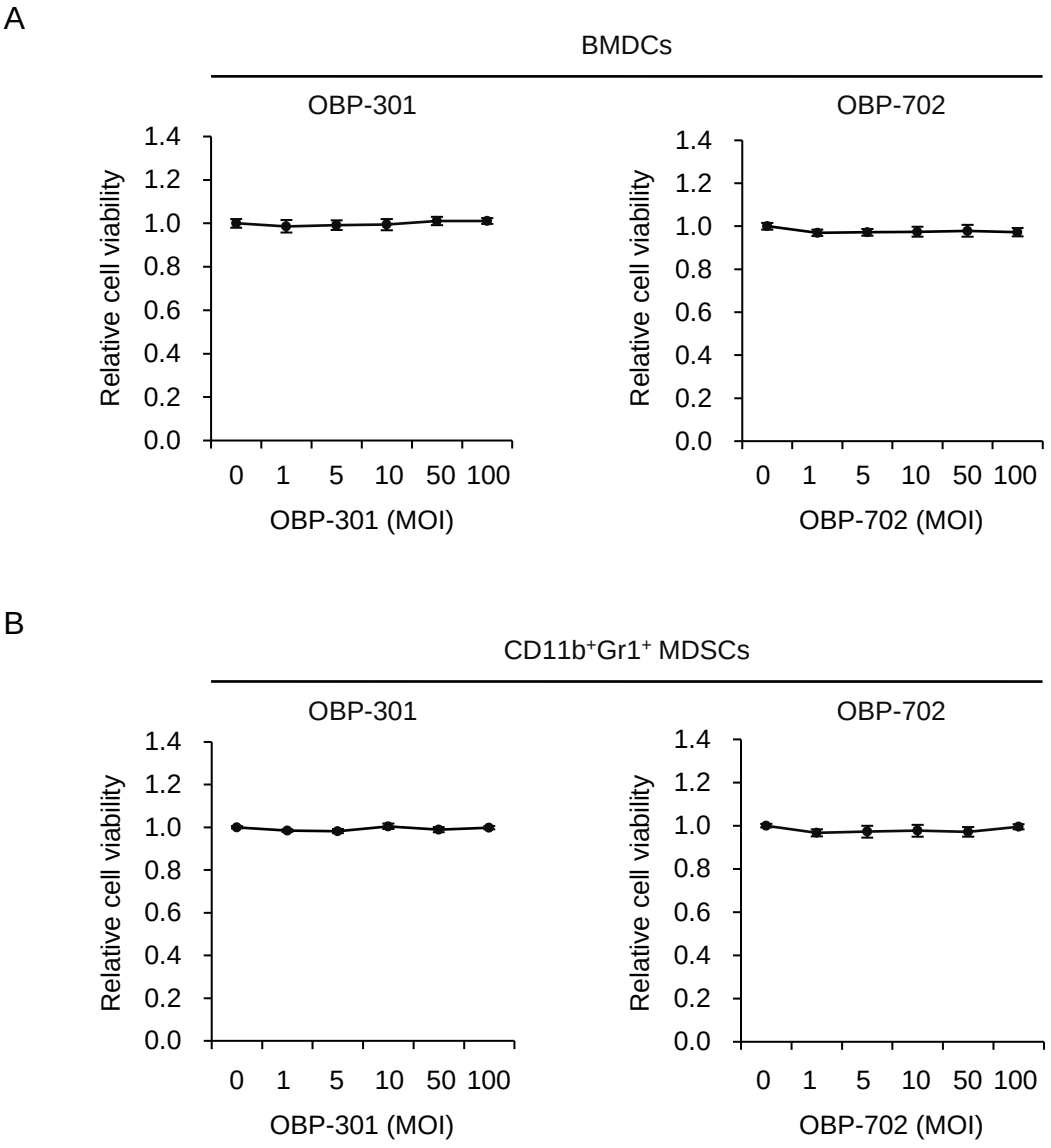

Supplementary Fig. S7. Relative viability of BMDCs and MDSCs after treatment with OBP-301 or OBP-702 for 3 days. A, **B**, BMDCs (**A**) or $CD11b^{+}Gr1^{+}$ MDSCs (**B**) seeded in 96-well plates were treated with OBP-301 or OBP-702 at the indicated MOIs for 72 h. Cell viability was quantified using the XTT assay and calculated relative to that of non-treated cells, which was set at 1.0. Cell viability data are expressed as mean ± SD (n = 5).

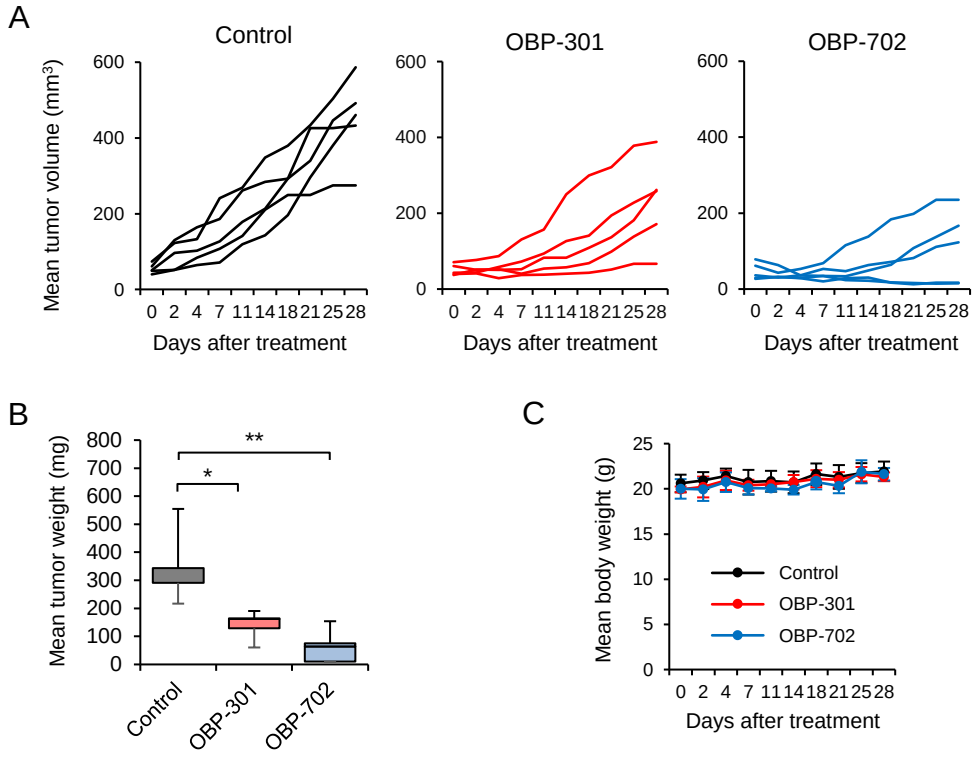

Supplementary Fig. S8. *In vivo* antitumor effect of OBP-301 and OBP-702 against GR PAN02 tumors. A, Individual tumor growth curves for GR PAN02 tumors treated with PBS, OBP-301 or OBP-702. **B**, Weight on day 28 of GR PAN02 tumors treated with PBS, OBP-301, or OBP-702. **C**, Change in body weight of mice bearing GR PAN02 tumors treated with PBS, OBP-301, or OBP-702. Data are expressed as mean ± SD (n = 5 in each group; *, $P < 0.05$; **, $P < 0.01$).

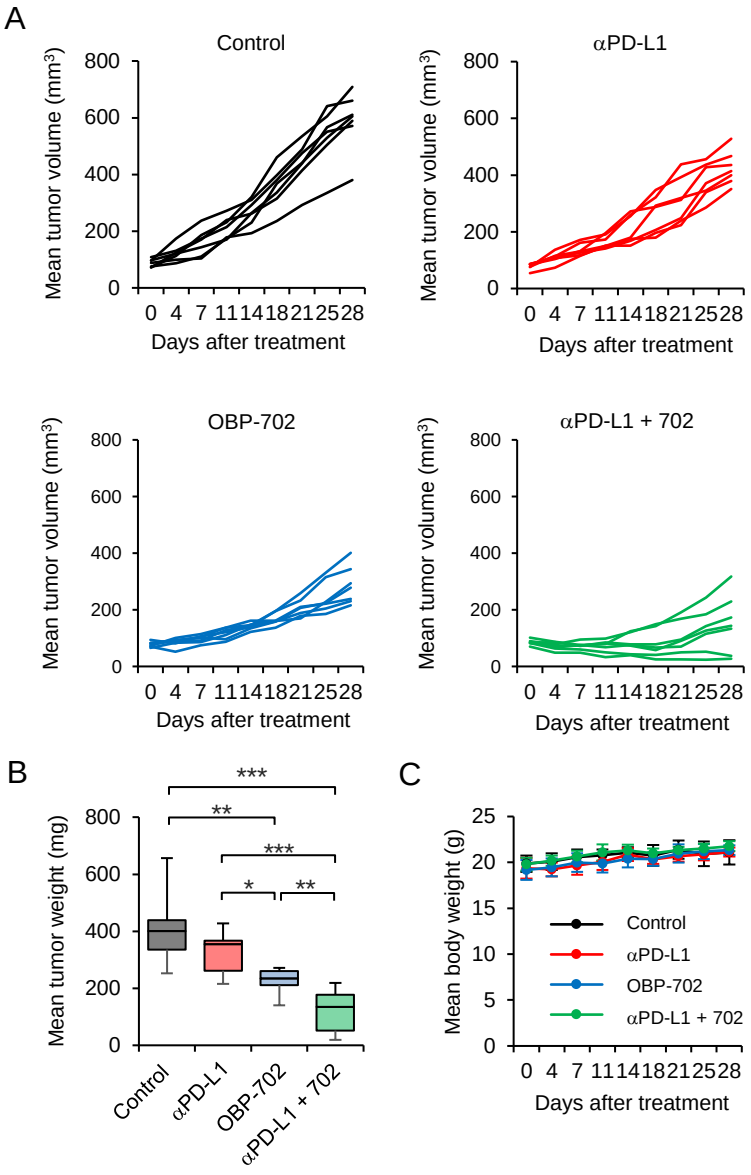

Supplementary Fig. S9. *In vivo* antitumor effect of PD-L1 blockade and OBP-702 in monotherapy or combination therapy against GR PAN02 tumors. A, Individual tumor growth curves for GR PAN02 tumors treated with anti-PD-L1 antibody, OBP-702, or combination. **B**, Weight on day 28 of GR PAN02 tumors treated with anti-PD-L1 antibody, OBP-702, or combination. **C**, Change in body weight of mice bearing GR PAN02 tumors treated with anti-PD-L1 antibody, OBP-702, or combination. Data are expressed as mean ± SD (n = 7 in each group; *, $P < 0.05$; **, $P < 0.01$; ***, $P < 0.001$).